Phase-space distributions and spectral properties for non-hydrogenic atoms in magnetic fields

1993 J. Phys. A: Math. Gen. 26 3187

(http://iopscience.iop.org/0305-4470/26/13/022)

J. Phys. A: Math. Gen. 26 (1993) 3187–3200. Printed in the UK

Phase-space distributions and spectral properties for non-hydrogenic atoms in magnetic fields

W Jans†, T S Monteiro‡, W Schweizer† and P A Dando‡

† Lehrstuhl fur Theoretische Astrophysik, Universitat Tübingen, D-7400 Tübingen, Federal Republic of Germany

‡ Department of Mathematics, Royal Holloway and Bedford New College, University of London, Egham, Surrey, TW20 0EX, UK

Received 9 November 1992, in final form 3 March 1993

Abstract. We present here the first study of the quantum phase-space behaviour (Wigner functions) for non-hydrogenic atoms in magnetic fields as well as a comprehensive study of spectral properties. We consider primarily an energy regime (scaled energy -0.5) where hydrogen is near-integrable and hydrogenic wavefunctions would be localized on tori. We find that the quantum energy level statistics for non-hydrogenic atoms are at the 'chaotic' (Wigner) limit. However, the quantum phase space distributions, contrary to what one would expect if the underlying classical motion were chaotic, remain dominated by torus-like structures. But the wavefunctions do explore a larger fraction of phase-space than in the hydrogenic case where, in the integrable regime, Wigner wavefunctions are generally localized on a single torus. Due to the non-semiclassical nature of the core they are localized on more than one torus; additional structures other than the tori are also present. Possible interpretations of the results in terms of models of the underlying classical dynamics are discussed.

1. Introduction

The problem of the hydrogen atom in a magnetic field remains one of the most rewarding case studies in the field of quantum chaology, i.e. the study of the behaviour of quantum systems whose classical counterparts are chaotic. The diamagnetic hydrogen atom is one of the simplest low-dimensional systems accessible to both experimental and theoretical study. More importantly though, it has a scaling property of energy which has permitted detailed comparisons between the classical and quantal dynamics. So it has been possible to carry out detailed quantitative tests of predictions from theories such as periodic orbit theory (Gutzwiller 1971, 1990, Balian and Bloch 1972) and random matrix theories using such calculations at fixed scaled energies. Over the last few years this system has been intensively studied both by means of experiment (Holle *et al* 1988) as well as classical and quantal calculations (for reviews see Hasegawa *et al* 1989).

There is now also a considerable body of experimental work available on non-hydrogenic Rydberg atoms in fixed magnetic fields (Gay *et al* 1980, Castro *et al* 1980). In 1990 Monteiro and Wunner presented a theoretical method for the calculation of quantum spectra at fixed scaled energies. More recently experimental work has been carried out on non-hydrogenic atoms at fixed scaled energies (Hogervorst 1992). But to date little work has been carried out on the influence of the non-hydrogenic core on the dynamics of the diamagnetic Rydberg atom. There have been no previous studies of the quantum behaviour in phase-space.

0305-4470/93/133187+14$07.50

Unfortunately, for non-hydrogenic atoms, even at fixed scaled energy, comparisons with the underlying classical behaviour are not straightforward, since the multi-electron core does not lend itself to a semiclassical description in any energy regime. In the hydrogen atom case, quantum phenomena such as the behaviour of the energy level statistics, Wigner functions or Fourier transforms of spectra are well correlated with the classical dynamics. We consider here the value of these quantum properties as indicators of classical regularity/chaos in the presence of a non-hydrogenic core and discuss possible approaches to the classical limit.

2. Theory

The classical Hamiltonian in atomic units, H′, for the hydrogen atom in a magnetic field aligned along the z axis takes the form

$$H' = E = (p'^2/2) - (1/r') + \tfrac{1}{8}\gamma^2\rho'^2 + \tfrac{1}{2}\gamma L'_{z'} \tag{1}$$

where r' represents the distance between the nucleus and electron, $\rho' = (r'^2 - z'^2)^{1/2}$ and γ represents the magnetic field strength in atomic units ($\gamma = B/2.35 \times 10^5$ T). The dynamical range of most interest corresponds to coulomb and diamagnetic terms of comparable magnitude and is a function of both magnetic field strength as well as the energy E. But by means of a coordinate transformation $r \to r'\gamma^{2/3}$, $p \to p'\gamma^{-1/3}$ the Hamiltonian may be brought to the form (here we consider only the case $L_z = 0$)

$$H = H'\gamma^{-2/3} = (p^2/2) - (1/r) + \tfrac{1}{8}\rho^2 = \epsilon. \tag{2}$$

Hence now the classical dynamics is dependent only on a single parameter, the scaled energy $\epsilon = E\gamma^{-2/3}$. For ϵ less than about -1, the motion is completely regular. As ϵ is increased though, phase space progressively fills up with chaotic orbits and above about $\epsilon = -0.1$ is almost completely ergodic.

It is also possible to compute *quantum* spectra for the hydrogen atom in a magnetic field at fixed scale energy (Friedrich and Wintgen 1989). Scaling coordinates as above and rearranging the Schrödinger equation from its usual form gives

$$(-1/r + \tfrac{1}{8}\rho^2 - \epsilon)\Psi = \gamma_i^{2/3}\tfrac{1}{2}\nabla^2\Psi. \tag{3}$$

It is then possible to obtain a set of eigenvalues $\{\gamma_i^{2/3}\}$ for fixed ϵ corresponding to a set of energies $E_i = \epsilon\gamma_i^{2/3}$. The field strength has not been entirely eliminated though. Effectively each E corresponds to a different value of Planck's constant, i.e. $\hbar \to \hbar\gamma^{1/3}$ since the commutation relation between momentum and position coordinates, in scaled coordinates becomes $[r, p] = i\hbar\gamma^{1/3}$. However, all the eigenvalues now correspond to a single classical regime. Phenomena such as spectral densities and quantum scars are now subject to constant, sinusoidal fluctuations which are easily identified by means of Fourier transforms. Hence connections between classical and quantum physics are considerably clarified. Problems encountered with analyses of unscaled spectra—such as sensitive dependence of Fourier transforms on spectral range—are eliminated.

In a previous work (Monteiro and Wunner 1990) (referred to as MW below) a theoretical method for calculating the spectra of highly excited ('Rydberg') non-hydrogenic atoms at *fixed scaled energy* was presented. For such atoms, the presence of the electronic core means

that the classical Hamiltonian no longer scales. However, the non-coulombic interactions are relatively short-ranged and the non-scaling part is only a few atomic units in extent while corresponding wavefunctions or classical orbits are thousands of atomic units across.

Each non-hydrogenic atom may be characterized by a set of quantum defects μ, dependent on the orbital angular momentum l. In MW, only model atoms with a single quantum defect in the $l = 1$ channel were considered. The magnetic field does not mix odd and even l, so this is a realistic approximation to the behaviour of many Rydberg atoms since $\mu \approx 0$ for $l \geqslant 3$.

Wavefunctions and eigenvalues were calculated by matching an inner region described by quantum defect theory with an outer hydrogenic region by means of an adaptation of R matrix theory as described in Monteiro and Wunner (1990).

Preliminary results presented in that study showed that both spectral modulations as well as energy level statistics for non-hydrogenic atoms at a given ϵ were sensitive to the value of the quantum defect, with the greatest discrepancy occurring for half integer values of μ. One possible explanation was to suggest that the differences were due to changes in stability of classical orbits.

In order to investigate these discrepancies we have carried out a study of the quantum phase-space properties of non-hydrogenic atoms as well as an extensive study of the spectral properties.

A study of a phase-space version of the wavefunction—the Wigner function—for the hydrogen atom was carried out by Schweizer *et al* (1992). The Wigner function $W(p, q)$ represents the Weyl transform of the wavefunction in configuration space $\Psi(q)$. For an N-dimensional system it is related to it as follows:

$$W(p, q) = 1/(2\pi)^N \int \Psi^*(q + \lambda/2)\Psi(q - \lambda/2) \exp(-ip\lambda)\, d\lambda. \tag{4}$$

The Wigner function is only one among several possible phase-space representations of the wavefunction (Hillery *et al* 1984). The Husimi distribution (Müller 1992) which is effectively a Gaussian smoothed version of $W(q, p)$, represents another suitable alternative and has also been applied to this problem.

In the case of the hydrogen atom, for $\epsilon = -0.5$ most wavefunctions are localized on tori associated with two stable periodic orbits: one representing motion perpendicular to the magnetic field, the other motion parallel to the magnetic field. Some wavefunctions are also localized near a fixed point and invariant manifolds associated with an unstable orbit which is near circular in shape. Figure 1 represents the corresponding classical Poincare surface of section (SOS) for $\epsilon = -0.5$. Semi-parabolic coordinates $u, v = (r \pm z)^{1/2}$ have been used in the classical calculation. The section in phase-space was taken through $u = 0$, so the figure represents the v, P_v plane.

The SOS shows that phase space is dominated by elliptic islands corresponding to the perpendicular and parallel stable periodic orbits mentioned above. Between them lies a separatrix and hyperbolic fixed points associated with the nearly circular orbit.

We have calculated Wigner functions at $\epsilon = -0.5$, for a set of non-hydrogenic atoms with quantum defects $0 < \mu < 1$ in the s $(l = 0)$ channel. A set of eigenstates $\{\Psi_i(r)\}$ all at a given fixed scaled energy, ϵ, and each associated with a different eigenvalue $\gamma_i^{2/3}$, for non-hydrogenic atoms were obtained in the form

$$\Psi_i(r) = \sum_k A_k^i \Psi_k(r) \tag{5}$$

i.e. as linear combinations of a set of eigenfunctions $\{\Psi_k\}$ obtained from diagonalization of the diamagnetic hydrogen Hamiltonian over an outer region ranging from an inner boundary

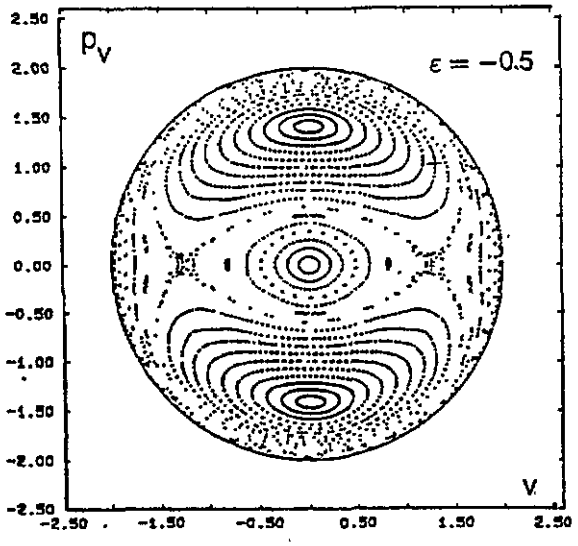

Figure 1. Classical Poincare surface of section for the hydrogen atom in a magnetic field for $\epsilon = -0.5$ in semiparabolic coordinates $u, v = (r \pm z)^{1/2}$. The section is taken through $u = 0$ and represents the v, P_v plane.

$r = a$ out to $r = \infty$. The expansion coefficients were then obtained by R matrix matching of Ψ to a quantum defect region at $r = a$.

The outer region eigenfunctions were calculated in terms of expansions over sturmian functions:

$$\Psi_k(r) = \sum_{n,l} C^k_{nl} S_{nl}(r) Y_{lm}(r). \tag{6}$$

By summing over k one could then obtain the Ψ_i in terms of expansions over sturmians, i.e.

$$\Psi_i(r) = \sum_{n,l} D^i_{nl} S_{nl}(r) Y_{lm}(r) \tag{7a}$$

where

$$D^i_{nl} = \sum_k A^i_k C^k_{nl} \tag{7b}$$

i.e. in similar form to that obtained for the usual solutions of the hydrogen atom by direct diagonalization of its Hamiltonian. Of course, strictly, unless $\mu = 0$ this expansion is only valid outside the non-hydrogenic core. However, the core is relatively small in extent compared with the wavefunction so when calculating phase-space distributions, (7*a*) was assumed to be valid over the whole range from $r = 0$ to ∞.

3. Results

Wigner functions were calculated by converting the wavefunction from spherical polar coordinates to semi-parabolic coordinates. Then a large two-dimensional fast Fourier

transform was carried out as described in Schweizer *et al* (1992). All the phase-space sections shown here were taken through $u = 0$.

The Wigner distributions cannot be positive everywhere (Hillery *et al* 1984). For any particular surface of section there are positive and negative contributions. In fact unlike Husimi distributions, the Wigners in addition to the major 'classical' structures such as tori have a background of quantum oscillatory structure both in phase-space as well as when one moves off the energy surface. These fringes have been investigated theoretically by Berry (1989).

The resulting Wigner distributions for a set of quantum levels ranging from the 180th level to the 195th level above the ground state for $\epsilon = -0.5$ are shown in figure 2 for $\mu = 0$ and in figure 3 for $\mu = 0.5$. The levels correspond to even parity with magnetic quantum number $m = 0$. The dark regions represent positive values for the Wigner functions, the white regions represent negative values, while the grey background represents zero enhancement in the Wigner distribution. The maximal values for the positive contributions for our $u = 0$ phase-space sections were typically of the same order of magnitude. However, for different wavefunctions they are between 1 and 75 times larger than the most negative values. The size of $\hbar$ in phase space is indicated by the square in the top left hand corner.

The size of the core region is not indicated in the surfaces of section since it is not a parameter of the calculation. In principle two different cores could produce similar quantum defects depending on the strength of the non-coulombic interaction. However, the physical size of the core region for a typical atom is of the order of a few atomic units, while the excited electronic states considered here are of the order of a couple of thousand units.

Figure 2 shows a subset of typical phase-space distributions which appear as a recurring pattern in the spectrum of the hydrogen atom. Levels 180, 183, 187–189, 191, 193 show examples of tori associated with the stable periodic orbit perpendicular to the field. Level 185 is localized about the fixed point corresponding to that orbit. Levels 181, 186, 190, 192 and 194 are localized about the elliptic fixed point and tori associated with the stable orbit parallel to the field.

Levels 182 and 195 on the other hand, are both localized predominantly near the separatrix of the motion; in configuration space the wavefunction would show a quantum scar nearly circular in shape corresponding to the unstable circular orbit. Since this orbit is unstable (albeit with a small Liapunov exponent) in the Gutzwiller series it provides only a sinusoidal modulation, rather than the harmonic oscillator-like level sets associated with stable orbits (Miller 1975). Hence levels scarred by this orbit fall near, though not exactly at integer multiples of the scaled action. Therefore, in addition to some weak fringe structures, it is not unexpected that states which are predominantly localized about the separatrix show features associated with the larger tori of the two stable orbits parallel and perpendicular to the magnetic field axis.

Figure 3 represents a set of Wigner functions for the most non-hydrogenic (half-integer value of μ) atom possible. It shows a much more complex pattern and illustrates most of the phase-space features characteristic of the non-hydrogenic behaviour.

In phase space one now sees that, unlike the hydrogenic case, the Wigner functions are no longer mainly localized about a single torus. Further, although torus-like structures akin to those found in the hydrogen atom case may be seen, they appear among other structures. Levels 180, 181, 186 and 193 show distributions where 'tori' and fixed points associated with different classical orbits (of the hydrogen atom) are present. It may be seen (by comparing with figure 2) that many of the non-hydrogenic Wigners in figure 3 are, to some degree, mixtures of nearby hydrogenic Wigners.

However, apart from the tori and separatrix of hydrogen, other features are also seen

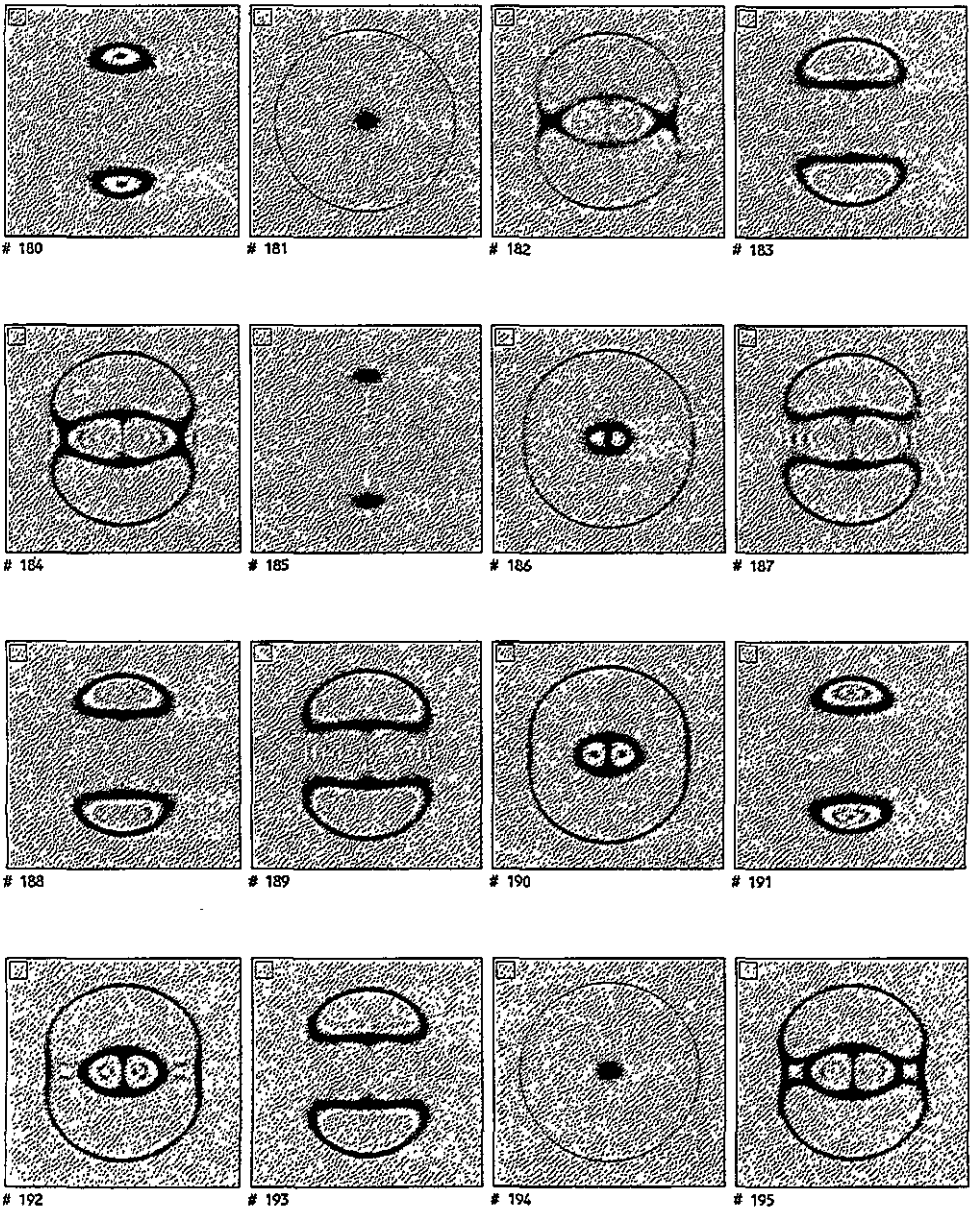

Figure 2. Set of Wigner function plots for quantum levels 180–195 of the hydrogen atom in a magnetic field for $\epsilon = -0.5$. The plots, for comparison with figure 1 are in the v, P_v plane through $u = 0$.

in figure 3. For example, levels 191 and 193 illustrate another phenomenon: not only are several 'tori' present, but they are also 'connected' by quantal phase-space structures. In addition, further structures similar in appearance with those one would find at high scaled energies, i.e. associated with hyperbolic fixed points and invariant manifolds, which were not present for hydrogen, are also seen in the non-hydrogenic states. Examples may be seen

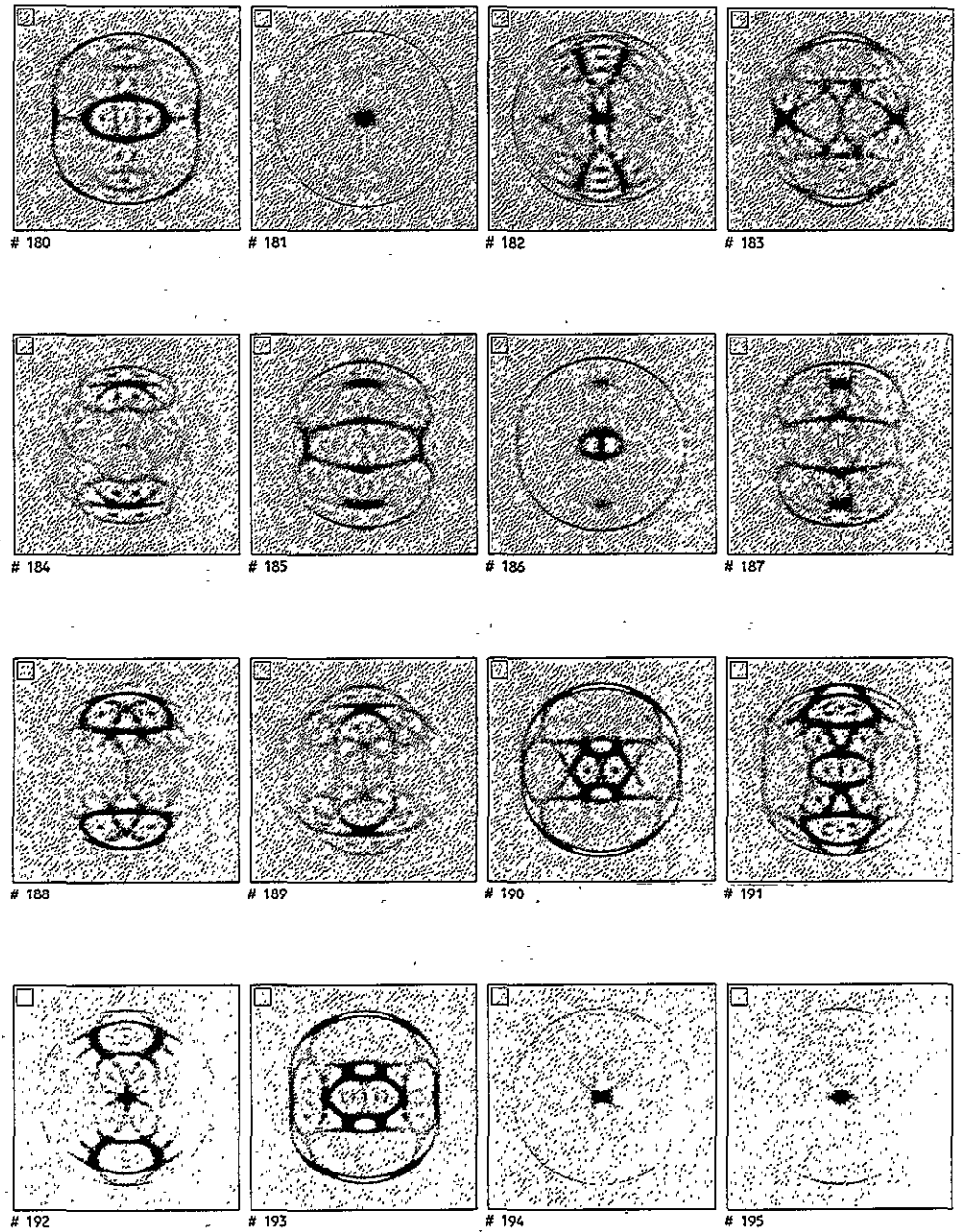

Figure 3. Set of Wigner function plots for quantum levels 180–195 of a model non-hydrogenic atom (i.e. $\mu = 0.5$) in a magnetic field for $\epsilon = -0.5$. The plots, for comparison with figure 1 are in the v, P_v plane through $u = 0$.

in levels 184 and 189 among others. A few levels such as 192 or 182 show no obvious sign of the original toroidal structure apparent in nearby hydrogenic states.

Wigner distributions for other non-zero quantum defects also display these features; in phase-space non-hydrogenic behaviour is clearly seen for $\mu = 0.1$, gradually intensifies up to $\mu = 0.5$, but then gradually decreases as μ tends to 1 because the quantum behaviour is

modulo 1 in the quantum defect as the latter represents a phase shift.

In sum, figure 3 shows that non-hydrogenic wavefunctions explore a considerably greater part of phase space than is the case for hydrogen. Phase-space is no longer clearly partitioned. If we were to consider lower intensities (by employing a logarithmic scale for figure 3) we would find an even more complex structure.

The non-hydrogenic Wigner functions are no longer restricted to tori. However, even for $\mu = 0.5$ they are qualitatively different from those associated with the truly 'chaotic' hydrogen atom for $\epsilon > -0.1$. In the latter case, the exponential proliferation of unstable periodic orbits gives quantum phase-space distributions a more complex and 'ergodic' appearance (though less so in the case of quantum states which are strongly scarred by predominantly one periodic orbit). Certainly there are no torus-like structures present.

We also considered here another signature of underlying classical chaos, the energy level statistics. In the limit of completely regular motion, or in the limit of completely chaotic dynamics, nearest neighbour spacings (NNS) distributions fall into universal classes, the former being associated with a Poisson distribution and the latter with what is termed a Wigner distribution (unrelated to the Wigner function studied above). Intermediate dynamics between regularity and chaos are not associated with universal distributions but instead have NNS distributions which depend on the details of the dynamics of the particular system under consideration.

Brody (1973) showed that the NNS could be fitted analytically by a functional form depending on a single parameter, Q, termed the Brody parameter. The Brody fit tends to the Poisson limit for $Q \to 0$ and to the Wigner limit for $Q \to 1$. The Brody parameter is roughly related to the fraction of classical phase-space occupied by chaotic orbits. But in the diamagnetic hydrogen case the quantum statistics can exhibit large deviations from this rule.

We have fitted sets of nearest neighbour distributions for different scaled energies to the analytical Brody form, which is shown below:

$$P(S) = \alpha(Q+1)S^{Q} \exp(-(\alpha S^{Q+1})) \tag{8}$$

where $P(S)$ represents the probability of nearest neighbours lying within an interval S of each other and

$$\alpha = [\Gamma\{(Q+2)/(Q+1)\}]^{Q+1}. \tag{9}$$

Figure 4 shows a set of plots of the Brody parameter (actually of $1 - Q$) against the scaled energy ϵ for a set of five different quantum defects. Then a value of 1 on the vertical axis corresponds to regular (Poisson) statistics while zero would correspond to 'chaotic' (Wigner) statistics. An example of a Brody fit to a set of nearest neighbours is also shown.

In the case of the hydrogen atom, the distribution would only be fully chaotic for $\epsilon > -0.13$ and is quite near the regular limit for $\epsilon = -0.5$. A remarkable feature, found by Hegerfeldt and Henneberg (1990) is the prominent resonance centred near $\epsilon = -0.32$. It occurs at a scaled energy where the important stable orbit perpendicular to the magnetic field has a rational winding number. In the semiclassical periodic orbit expansion of Gutzwiller this effectively means that the coefficient corresponding to the second traversal of this orbit becomes infinite (Honig and Wintgen 1989). The resulting quantum energy level spectrum is then strongly modulated by the perpendicular orbit—or rather by sets of harmonic oscillator levels. Hence the NNS statistics veer sharply towards the regular limit.

If we now consider the statistics due to non-hydrogenic atoms, we find that their statistics lie nearer the Wigner limit, most so for $\mu = 0.5$. In fact, for $\mu = 0.5$ the NNS distribution

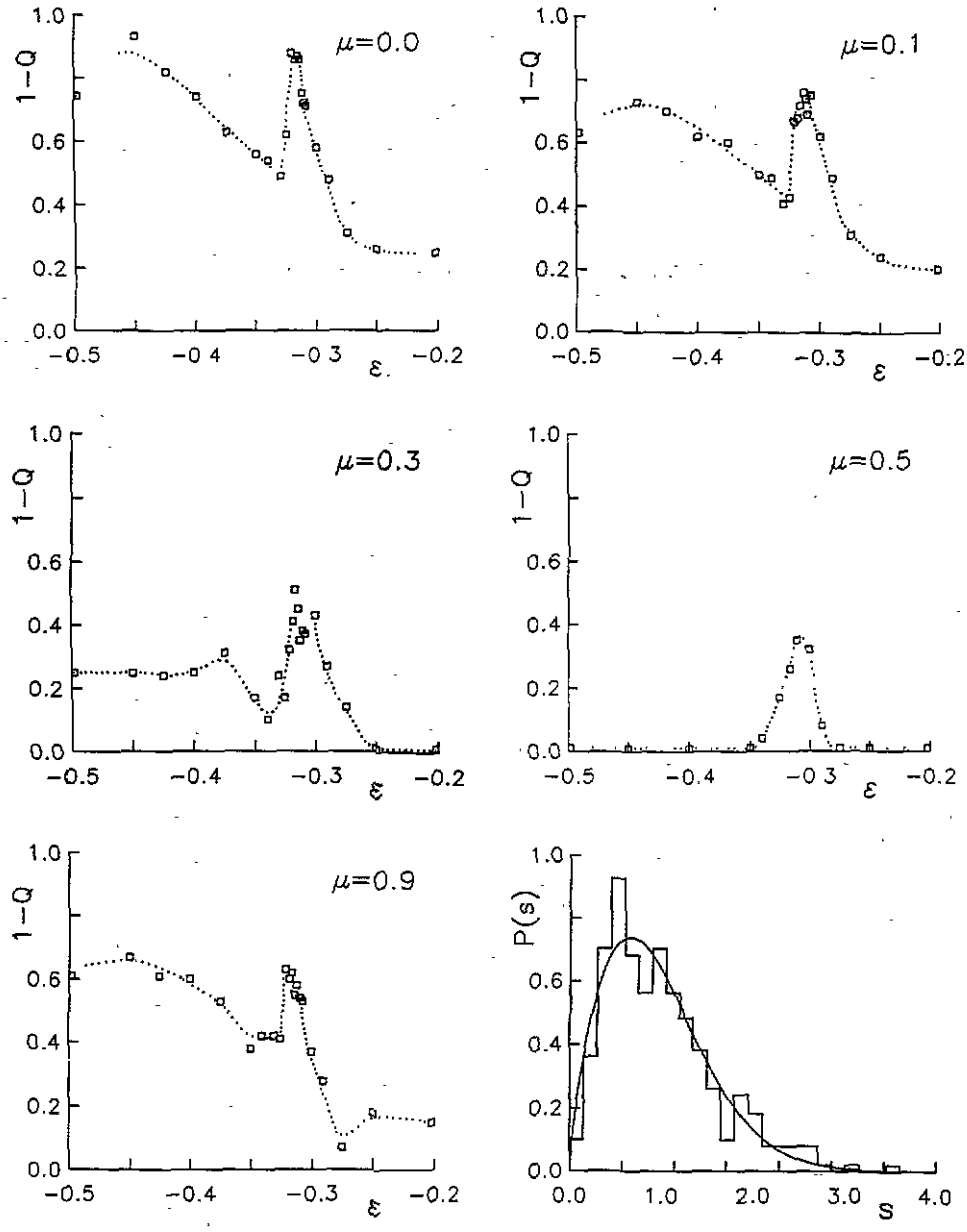

Figure 4. Plots of $1-Q$ (where Q are Brody parameters) against scaled energy for a set of quantum defects. An example of the fit obtained at $\epsilon = -0.4$, $\mu = 0.3$ is also shown.

is already at the $Q = 1$ limit for $\epsilon = -0.5$. Other quantum defects have Brody parameters intermediate between the values found for $\mu = 0$ and $\mu = 0.5$.

However, the resonance is prominent for all quantum defects, including $\mu = 0.5$. The explanation for the resonance, which relies on the Gutzwiller formula, strictly only applies to a stable orbit which is characterized by a rational winding number. Hence we infer from the level statistics that the perpendicular orbit is stable for $\mu = 0.5$ and $\epsilon = -0.32$.

We also considered another statistical indicator, the spectral rigidity. The same

qualitative behaviour was encountered, with the non-hydrogenic statistics much nearer the GOE (Gaussian orthogonal ensemble) limit (Bohigas and Giannoni 1984), particularly for $\mu = 0.5$, but with the resonance at $\epsilon = -0.32$ clearly seen for all quantum defects.

In Monteiro and Wunner (1990) we analysed modulations of the photoabsorption spectrum and their dependence on the quantum defect. It was found that the height of the Fourier transform peaks of the photoabsorption spectrum depend strongly on the quantum defect. Spectra with $\mu = 0.5$ had Fourier transform peaks which were present at the same classical scaled action as those for hydrogen, but with lower heights. The one exception found in the limited sample considered there was of a cluster of peaks for $\epsilon = -0.3$ which were only present for $\mu \neq 0$ and did not appear to correspond to any known hydrogenic orbits.

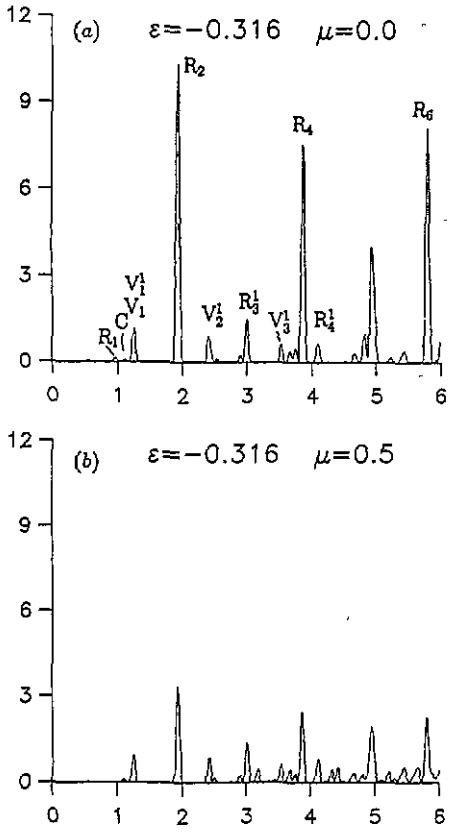

Figure 5. Fourier transformed energy level spectra at $\epsilon = -0.316$ for positive parity, $m = 0$ for (*a*) $\mu = 0$ (*b*) $\mu = 0.5$.

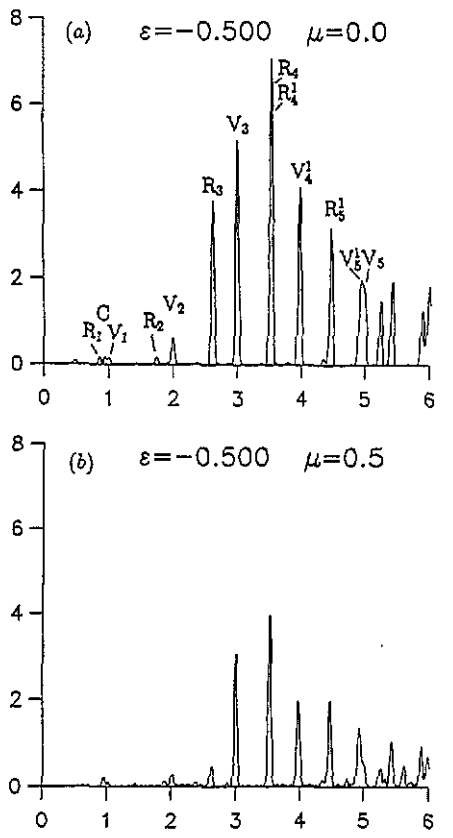

Figure 6. Fourier transformed energy level spectra at $\epsilon = -0.5$ for positive parity, $m = 0$ for (*a*) $\mu = 0$ (*b*) $\mu = 0.5$.

Here we obtained also a set of Fourier transforms of the level densities. It should be noted that the eigenvalues we calculated are $\gamma^{2/3}$, whereas the transformation is with respect to $\gamma^{-1/3}$. According to standard periodic orbit theory the heights of the peaks in the transforms are related to the Liapunov exponent of unstable periodic orbits—or, in the case of a stable orbit the heights of the peaks (and hence the coefficient of the Gutzwiller expansion) are related to the winding number of the periodic orbit in question.

The results are displayed in figures 5–7 for hydrogen and quantum defect 0.5. the horizontal axis corresponds to the gamma-scaled action ($\gamma^{1/3}$ times the action in atomic units). The transforms employed quantum levels ranging from effective principal quantum number 18 through to effective quantum number 45–60 depending on the scaled energy (300–350 levels for each transform).

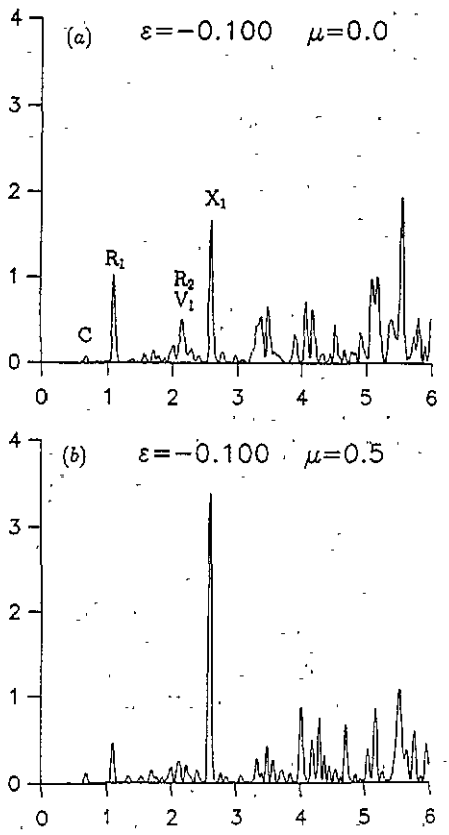

Figure 7. Fourier transformed energy level spectra at $\epsilon = -0.1$ for positive parity, $m = 1$ for (*a*) $\mu = 0$ (*b*) $\mu = 0.5$.

Figure 5(*a*) and 5(*b*) show Fourier transforms of energy level spectra for $\mu = 0$ and $\mu = 0.5$ near the resonance energy—here $\epsilon = -0.316$. The transform corresponds to positive parity and $m = 0$. In both spectra, the classical orbits corresponding to each individual peak have been identified using the nomenclature of Holle *et al* (1988). It may be seen that the hydrogen atom transform (figure 5(*a*)) is dominated by a set of large peaks indicated by R_2, R_4, R_6. These correspond to an even number of traversals of the perpendicular orbit, R_1. Figure 5(*b*) shows that the strong resonance is attenuated but is still present for $\mu = 0.5$.

Figure 6(*a*) and 6(*b*) show a similar set of results (even parity, $m = 0$) but for $\epsilon = -0.5$. This spectrum is dominated by the three periodic orbits R_1 (perpendicular to the field), V_1 (parallel to the field) and C (circular). There is also a set of prominent peaks corresponding to the nth traversals of these orbits. Figure 6(*b*) shows that in the $\mu = 0.5$ case, the heights due to the harmonics of the basic orbits are drastically reduced. Miller (1975) showed that stable orbits like R_1 and V_1 give rise to sets of harmonic oscillator levels equidistantly spaced. This gives the quantum level spectrum (plotted on a $\gamma^{-1/3}$ scale) a highly ordered

appearance. For $\mu = 0.5$ this is no longer the case. These oscillator levels are perturbed and are no longer equidistant from each other, hence the Fourier transform of such a spectrum will produce weaker peaks.

Finally, figure 7(*a*) and 7(*b*) show some uncharacteristic behaviour found for $\epsilon = -0.1$ (in this case for odd l values, $m = 1$). At this energy there is a peak which is prominent for both $\mu = 0$ and $\mu = 0.5$. However, it is significantly *stronger* for $\mu = 0.5$. It is labelled X_1, since it coincides with an asymmetric 'exotic' orbit identified by Holle *et al* (1988). These exotic orbits appear suddenly at singular points—in fact closer inspection of the classical behaviour shows that the peak actually corresponds to a *pair* of asymmetric orbits. There is no clear reason for why this peak should be enhanced for non-hydrogenic atoms. Similar behaviour was found for another 'exotic' (X_3 in Holle *et al* 1988). One could note that these peaks in the hydrogenic case become more prominent at energies above the birfurcation point where they are born. Hence one plausible explanation might be that the non-hydrogenic core has in effect shifted the position of this bifurcation point.

4. Discussion

So can one interpret the results, as suggested in Monteiro and Wunner (1990), in terms of a destabilization of the periodic orbits? For the diamagnetic non-hydrogenic atom, propagation within the core region will not tend to the semiclassical limit even at high energies. So there is no straightforward classical limit as is available in the hydrogen atom case.

For the hydrogen atom, much may be inferred about the underlying classical dynamics from standard indicators of classical chaos such as the energy level statistics or spectral modulations. The statistics are broadly correlated with the fraction of phase-space occupied by chaotic orbits—though there are large deviations such as at the resonance. The height of the spectral modulations is to a good approximation given by the stability parameters. The phase-space distributions in the near-integrable regime are localized about a single torus with a well defined quantization condition.

In the non-hydrogenic case, we find that these 'standard indicators' are very little use as they point in contradictory directions. Even for $\epsilon = -0.5$, the statistics are at the fully 'chaotic' limit. Yet phase space remains dominated by tori (albeit in a complex manner). In most cases the amplitude of the Fourier transform peaks in figures 5–7 is significantly reduced in the presence of a quantum defect, but it is clear that in the Gutzwiller formula they may no longer be approximately fitted by a simple form (*sine* or *sinh*) of a small set of stability parameters and a more complex form for the prefactor is involved.

One interpretation of the results is in terms of the scattering model of Du and Delos (1988a, b) and Gao and Delos (1992): semiclassical waves propagate along the classical periodic orbits of the hydrogen atom; on encountering the core they are quantum mechanically scattered with phaseshifts given by the quantum defects and amplitude is redistributed into the other hydrogenic periodic orbits. In this model the classical dynamics remains hydrogenic, but semiclassical waves do not propagate indefinitely along a given stable periodic orbit. This model would result in a different form for the prefactor in the Gutzwiller formula. It would not, however, account for the additional modulations found in Monteiro and Wunner (1990) or for shifts in bifurcation points. The implementation of the model by Gao and Delos (1992) on the sodium atom in an electric field produced only a small shift in the spectral modulations. Work is in progress to test a similar model for diamagnetic non-hydrogenic atoms and to obtain a more appropriate form for the amplitude in the Gutzwiller formula.

Another approach to a classical limit of sorts involves replacing the core by a one-electron model-potential which reproduces accurately the quantum spectrum. Such potentials are readily available for the alkali atoms. We are undertaking calculations on this system which will be published in due course. Preliminary results indicate that a single orbit will fill the whole of phase space by means of successive collisions with the core; i.e. a single orbit will hop from one torus to another following scattering by the core. In between, trajectories are restricted to a given torus.

Finally one must also consider quantum mechanical dependence on the size of $\hbar$—as suggested in Monteiro and Wunner (1990). The results presented here are qualitatively similar at different spectral ranges (corresponding to different effective sizes of $\hbar$). In particular, Wigner functions near levels 300 were also obtained. The amplitudes of Fourier transforms are with few exceptions reduced in the presence of a quantum defect, regardless of the energy range used for a transform. However, a quantitative test for the spectral modulations will have to await the implementation of a scattering model.

5. Conclusion

In conclusion, although the model non-hydrogenic atom shows some 'quantum signatures' of underlying unstable classical dynamics, increasingly so as μ tends to half-integer numbers, the system is far from ergodic. The probable interpretation is that classical orbits will tend to follow a torus for a limited period of time, until they are disturbed by a collision with the core. This is consistent with preliminary classical calculations using a model potential to describe non-hydrogenic atoms as well as the scattering model of Du and Delos (1988a, b). There it was found that classical orbits, after lingering in the vicinity of a torus for a limited time, are able to 'jump' to another, completely different torus following scattering by the core. Hence although the classical trajectories may in the long term explore most of phase space, their progress is quite different from an ergodic trajectory as a given orbit fills phase space by exploring different tori in turn and relying on the fact that the tori fill phase space densely. Quantum states on the other hand are restricted to the subset of tori which satisfy appropriate quantization conditions, given the scaled action corresponding to a particular state. Hence the Wigner functions remain dominated by, typically, two or three tori.

Acknowledgments

The authors acknowledge the support received from the UK–Germany Academic Research Collaboration Programme and SERC. The authors are grateful to M Schaich, K Taylor, G Wunner and H Ruder for stimulating discussions.

References

Balian R and Bloch C 1972 *Ann. Phys., NY* **69** 76

Berry M V 1989 *Proc. R. Soc.* A **423** 219

Bohigas O and Giannoni M J 1984 *Mathematical and Computational Methods in Nuclear Physics, Proceedings, Granada 1983, Lecture Notes in Physics 209* (Berlin: Springer)

Brody T A 1973 *Lett. Nuovo Cim.* **7** 482

Castro J C, Zimmerman M L, Hulet R G and Kleppner D 1980 *Phys. Rev. Lett.* **15** 1780

Du M L and Delos J B 1988a *Phys. Rev.* A **38** 1896

—— 1988b *Phys. Rev.* A **38** 1913
Friedrich H and Wintgen D 1989 *Phys. Rep.* **183** 37
Gao J and Delos J B 1992 *Phys. Rev.* A **46** 1455
Gay J C, Delande D and Biraben F 1980 *J. Phys. B: At. Mol. Phys.* **13** L720
Gutzwiller M C 1971 *J. Math. Phys.* **12** 343
Gutzwiller M C 1990 *Chaos in Classical and Quantum Mechanics* (New York: Springer)
Hasegawa H, Robnik M and Wunner G 1989 *Progress of theoretical physics supplement published by the Physical Society of Japan* **98** 198
Hegerfeldt G C and Henneberg R 1990 *Phys. Rev.* A **41** 1161
Hillery M, O'Connell R F, Scully M O and Wigner E P 1984 *Phys. Rep.* **106** 121
Hogervorst 1992 private communication
Holle A, Main J, Wiebusch G, Rottke H and Welge K H 1988 *Phys. Rev. Lett.* **61** 161
Honig A and Wintgen D 1989 *Phys. Rev.* A **39** 5642
Miller W H 1975 *J. Chem. Phys.* **663** 996
Monteiro T S and Wunner G 1990 *Phys. Rev. Lett.* **65** 1100
Muller K 1992 *PhD Thesis* University of Heidelberg
Schweizer W, Schaich M, Jans W, Wunner G and Ruder H 1992 *J. Phys. A: Math. Gen.* preprint